VIBRATION OF AND ACOUSTIC RADIATION FROM A PANEL EXCITED BY ADVERSE PRESSURE GRADIENT FLOW

by

Yi Mason Chang

and

Patrick Leehey

Report No. 70208-12

May 1976

This research was carried out under the Naval Ship Systems Command General Hydromechanics Research Program Subproject SR 009 01 01, administered by the David W. Taylor Naval Ship Research and Development Center Contract N00014-67-A-0204-0003

Massachusetts Institute of Technology
Cambridge, Massachusetts 02139

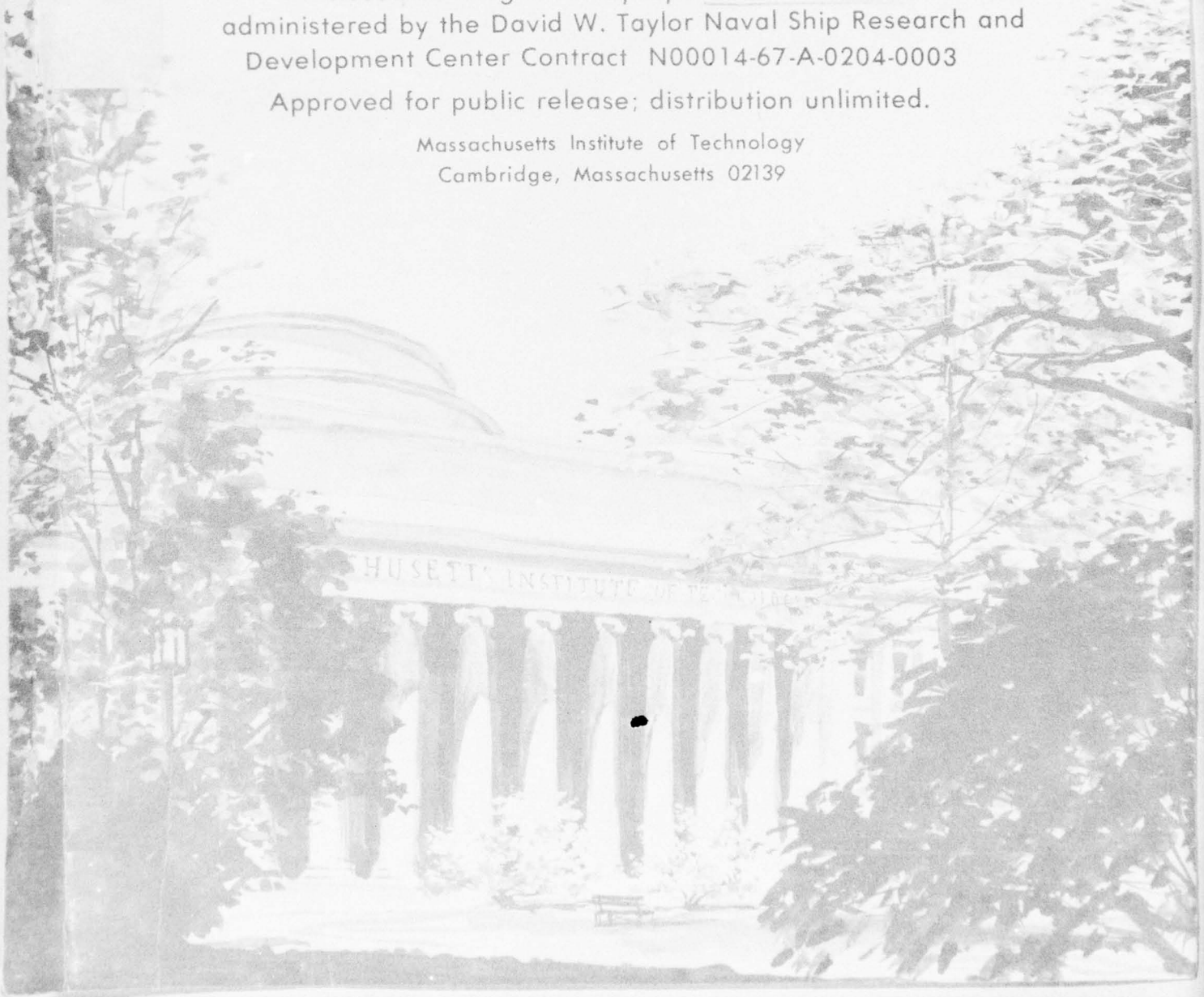

VIBRATION OF AND ACOUSTIC RADIATION FROM A PANEL EXCITED BY ADVERSE PRESSURE GRADIENT FLOW

by

Yi Mason Chang
and
Patrick Leehey

Report No. 70208-12

May 1976

This research was carried out under the Naval Sea Systems Command General Hydromechanics Research Program Subproject SR009 01 01, administered by the David W. Taylor Naval Ship Research and Development Center Contract N00014-67-A-0204-0002.

Approved for public release; distribution umlimited.

Acoustics and Vibration Laboratory
Massachusetts Institute of Technology
Cambridge, Massachusetts 02139

UNCLASSIFIED

SECURITY CLASSIFICATION OF THIS PAGE *(When Data Entered)*

REPORT DOCUMENTATION PAGE

READ INSTRUCTIONS BEFORE COMPLETING FORM

1. REPORT NUMBER: Acoustics & Vibration Lab. ✓ / AVL-70208-12 (14)
2. GOVT ACCESSION NO.
3. RECIPIENT'S CATALOG NUMBER

4. TITLE *(and Subtitle)* (6): Vibration of and Acoustic Radiation from a Panel Excited by Adverse Pressure Gradient Flow. ✓
5. TYPE OF REPORT & PERIOD COVERED: October 1974 through 31 March 1975.
6. PERFORMING ORG. REPORT NUMBER

7. AUTHOR(s) (10): Yi Mason/Chang and Patrick/Leehey
8. CONTRACT OR GRANT NUMBER(s) (15): N00014-67-A-0204-0002

9. PERFORMING ORGANIZATION NAME AND ADDRESS
Massachusetts Institute of Technology
Cambridge, Massachusetts 02139
10. PROGRAM ELEMENT, PROJECT, TASK AREA & WORK UNIT NUMBERS (12) 36p.

11. CONTROLLING OFFICE NAME AND ADDRESS
David W. Taylor Naval Ship Research and Development Ctr., Bethesda, MD 20034
12. REPORT DATE (11): May 1976
13. NUMBER OF PAGES: 33

14. MONITORING AGENCY NAME & ADDRESS *(if different from Controlling Office)*
15. SECURITY CLASS. *(of this report)*: Unclassified
15a. DECLASSIFICATION/DOWNGRADING SCHEDULE

16. DISTRIBUTION STATEMENT *(of this Report)*
Approved for public release; distribution umlimited.
(9) Rept. for Oct 74 - 31 Mar 75,

17. DISTRIBUTION STATEMENT *(of the abstract entered in Block 20, if different from Report)*
(16) SR0D901
(17) SR009101

18. SUPPLEMENTARY NOTES

19. KEY WORDS *(Continue on reverse side if necessary and identify by block number)*
Boundary Layer Noise
Plate Vibration
Acoustic Radiation
Wall Pressure Fluctuation
Adverse Pressure Gradient

20. ABSTRACT *(Continue on reverse side if necessary and identify by block number)*

Flow with uniform adverse pressure gradient was created over the surface of a steel test plate. Vibration velocity levels on the plate and acoustic radiation from the plate were measured and compared with theoretical estimates. The measured vibration levels agree with theory for frequencies above those

(continued)

DD FORM 1 JAN 73 1473 EDITION OF 1 NOV 65 IS OBSOLETE
S/N 0102-014-6601

UNCLASSIFIED

SECURITY CLASSIFICATION OF THIS PAGE (When Data Entered)

405 028

UNCLASSIFIED

for hydrodynamic coincidence. Below these frequencies theoretical predictions of radiated sound power, based on measured vibration levels, are too low. Possible reasons for these compensating errors are discussed.

UNCLASSIFIED

VIBRATION OF AND ACOUSTIC RADIATION FROM A PANEL EXCITED BY ADVERSE PRESSURE GRADIENT FLOW

by

Yi Mason Chang and Patrick Leehey

ABSTRACT

Flow with uniform adverse pressure gradient was created over the surface of a steel test plate. Vibration velocity levels on the plate and acoustic radiation from the plate were measured and compared with theoretical estimates. The measured vibration levels agree with theory for frequencies above those for hydrodynamic coincidence. Below these frequencies theoretical predictions of vibration levels are too high, but theoretical predictions of radiated sound power, based on measured vibration levels, are too low. Possible reasons for these compensating errors are discussed.

TABLE OF CONTENTS

LIST OF FIGURES

I. INTRODUCTION

Several previous studies have dealt with the analysis and measurement of the radiation of sound by plates and membranes excited by turbulent boundary layers. However, these studies have dealt only with turbulent boundary layers with negligible pressure gradients. Burton (1973) has shown that pressure gradients affect the flow field considerably, particularly in the case of an adverse pressure gradient flow. Burton's study was on a boundary layer with severe streamwise nonhomogeneity (shown by the shape factor, $H = \delta^*/\theta$). In this present work, we studied the effect of a boundary layer with adverse pressure gradient on the response of and the radiation from thin plates. However, here, the boundary layer has only mild streamwise nonhomogeneity. The following is a description of the work we have done and the findings we obtained.

II. DESCRIPTION OF THE TEST SETUP

All experiments were performed in the subsonic low-noise, low-turbulence wind tunnel in the Acoustic and Vibration Laboratory of the Massachusetts Institute of Technology. A complete description of this wind tunnel was provided by Hanson (1969). In order to create an adverse pressure gradient, the bottom wall of the wind tunnel was curved as shown in Fig. 2.1. This curved wall has a straight part over which a nearly uniform adverse pressure gradient is imposed on the flow. The test section was placed at the middle of the straight part of the curved wall.

A 3/4-inch thick plexiglass plate was mounted flush in the test section of the bottom wall to permit measurement of flow characteristics. Then a steel test plate of dimensions 11" x 13"

and a thickness of .003" replaced the plexiglass plate, and measurements were made of the sound power radiated into the airtight blockhouse surrounding the test section from turbulent boundary layer excitation on the plate. The plexiglass plate was used again in the test section during measurement of the background noise level in the blockhouse. The wind tunnel duct walls, including the curved bottom wall, were sand-loaded to reduce the vibration of, and hence the noise radiation from, the ducting.

In order to reduce the in-plane tension induced by the static pressure difference across the steel testing plate, pressure release holes were provided on the top wall of the wind tunnel. Steel wool was inserted into these holes to suppress whistling.

III. CHARACTERISTICS OF THE FLOW

A right-hand coordinate system is adopted with X_1 being the streamwise coordinate, X_2 being the normal coordinate pointing into the flow, and X_3 being the lateral coordinate. The 11" side of the plate is parallel to the X_1-direction. The origin was set at the midpoint of the upstream edge. The non-dimensional streamwise variable, ξ, has been defined by $dX_1 = \delta^*(X_1)d\xi$, where $\delta^*(X_1)$ is the local displacement thickness and $\xi = 0$ when $X_1 = 0$.

In measuring the mean flow properties, we mounted flush a 3/4-inch thick plexiglass plate in the test section. On this plexiglass plate, several test stations were used. The locations of these stations are illustrated in Fig. 3.1.

For the experiment, we ran the wind tunnel at two speeds.

The lower speed corresponds to a mean flow velocity, U_∞, at near 28 m/sec. The higher speed corresponds to a U_∞at near 45 m/sec.

Fig. 3.2 shows measured static pressure profiles along the X_1-direction. Boundary layer velocity profiles along the X_2-direction at three test stations and at two flow speeds are shown in Fig. 3.3. Mean flow velocity profiles at these stations and speeds are plotted in Fig. 3.4. The mean flow velocity, U_∞, is shown in Fig. 3.5. Based on these data, the displacement thickness and the momentum thickness were calculated and are illustrated in Fig. 3.6.

Wall pressure spectra, $\Phi(\omega)$, are shown in Fig. 3.7, and these are compared with results of Blake (1970) and Burton (1973).

Figure 3.8 shows longitudinal cross-spectral densities of wall pressure, which are compared with Schloemer's (1966) data. Figure 3.9 shows narrow band convection velocities.

IV. COMPARISON OF PANEL VIBRATION VELOCITY LEVELS COMPUTED FROM WALL PRESSURE STATISTICS WITH MEASURED LEVELS

Assuming that the exciting pressure field is spatially homogeneous in the plane of the wall, Davies (1971) derived the spectral density of the panel vibration velocity in the form,

$$S_v(\omega) = \frac{\pi\, n_s}{A_p\, 2\omega\, m_p^2\, \eta} \langle \Phi_{mn} \rangle \quad ,$$

where A_p = area of panel,

m_p = mass per unit area of the panel,

n_s = frequency mode density of the panel,

η = modal loss factor, including both mechanical and acoustical losses, and

$\langle \phi_{mn} \rangle$ = average modal wall pressure spectral density.

Davies also showed that

$$\langle \phi_{mn} \rangle = \Phi(\omega) \frac{4\alpha_1 \alpha_3 U_c^2}{\pi \omega^2} \int_0^{\pi/2} \left\{ \frac{1}{1+\alpha_1^2(1-\gamma\cos\theta)^2} + \frac{1}{1+\alpha_1^2(1+\gamma\cos\theta)^2} \right\} \frac{1}{1+\alpha_3^2\gamma^2\sin^2\theta} \, d\theta$$

with $\Phi(\omega)$ = wall pressure spectral density

U_c = convection velocity

$\gamma = (\omega_h/\omega)^{1/2}$ and $\omega_h = U_c^2(m_p/D)^{1/2}$,

and D is the panel flexural rigidity. The dimensionless constants α_1 and α_3 describe the spatial decay of the pressure field, for Davies used the model for cross-spectral density proposed by Corcos (1963), namely,

$$\Phi(\underline{r},\omega) = \Phi(\omega) \exp\left[-\frac{|\omega r_1|}{\alpha_1 U_c} - \frac{|\omega r_3|}{\alpha_3 U_c} - \frac{i\omega r_1}{U_c}\right]$$

Davies made a rough approximation for the integral used in the expression for $\langle \phi_{mn} \rangle$. We improved it by doing the integral numerically, using the Romberg quadrature technique. The vibration levels so computed are illustrated in Fig. 4.2.

For the present computations, $\Phi(\omega)$ was taken as the average value for the six stations shown on Fig. 3.7. The longitudinal decay parameter was taken as $\alpha = 8$ from the average of the data for three stations as shown on Fig. 3.8. Similarly, a convection velocity $U_c = 0.6U_\infty$ was taken as the average from the data at three stations as shown on Fig. 3.9. The lateral decay parameter was not measured, but was taken as $\alpha_3 = 1.1$ from Burton (1973). Burton showed that this parameter was not sensitive to an adverse pressure gradient. The plate modal loss factor was taken from the data in Fig. 4.1.

The power spectral densities of the vibration levels of the panel reduced from the third octave band levels are shown in Fig. 4.2. We see that the experimentally measured vibration levels agree with the theoretically predicted levels at frequencies higher than the hydrodynamic coincidence frequency, f_h. Note that f_h is 415 Hz for the $U_\infty \simeq 28$ m/sec case, and that f_h is 1050 Hz for the $U_\infty \simeq 45$ m/sec case. However, the predicted levels are 6 to 10 dB higher than the measured levels at frequencies below f_h.

V. COMPARISON OF MEASURED AND PREDICTED SOUND POWER LEVELS

The average modal radiation coefficients were computed by making use of the assumption of equipartition of energy among the modes (see Davies (1971)).

From these average modal radiation coefficients and the measured vibration levels of the test plate, we predicted the radiated sound power levels for the plate, as shown in Fig. 4.3. These are compared with the direct measurements of radiated sound power levels reduced from the sound pressure levels using the room constants. The room constants were determined using the acoustic loss factor η_b measured in one-third octave bands (Fig. 4.4).

It is important to note that in contrast to the comparisons of vibration levels presented in Fig. 4.2, the comparison of sound power levels in Fig. 4.3 shows the measured levels exceeding the predicted levels by from 6 to 10 dB in the lower frequency ranges. The measured data in Fig. 4.3 could not be extended beyond the 800 Hz band for $U_\infty = 28$ m/sec and the 1600 Hz band for $U_\infty = 45$ m/sec because of background noise limitations.

VI. DISCUSSION

One possible explanation for the theoretical vibration levels exceeding measured levels at frequencies below hydrodynamic coincidence may lie in the use of a Corcos model to represent the wall pressure statistics. Recently, Martin and Leehey (1976) have found that such a model describes the convective ridge well, but for the zero gradient case overpredicts low wave number components at a given frequency by as much as 13 dB. Such components become important in determining plate vibratory response at frequencies significantly below that for hydrodynamic coincidence, even in this analysis which computes only the vibratory response of resonant modes.

On the other hand, the measured sound power levels exceed those predicted from measured vibration levels. Since these predictions were based upon computed radiation efficiencies of resonant modes alone, it is possible that significant contributions to a particular frequency band are made from modes whose resonant frequencies lie much lower. Such modes have high radiation efficiencies, but contribute little to the vibration spectrum. Thus the prediction scheme used could significantly underestimate the radiated sound power.

The method of analysis used here is essentially that of Davies (1971) except that he made a direct prediction of the radiated sound power without making the intermediate calculation of the vibration spectrum. Thus he effectively used the theoretical rather than the experimental vibration spectrum to compute the radiated sound power. His computed values of sound power agreed quite well with experiment. Our results, however, suggest

that this agreement may have been due to a fortuitous error cancellation.

Our analysis ignores the streamwise variation of the properties of the wall pressure field. For a severe adverse pressure gradient this spatial inhomogeneity can be quite important. Its effect is likely to cause a significant increase in low wave number components of the wall pressure field. The adverse pressure gradient produced in these experiments, however, was probably not large enough for such effects to be important.

REFERENCES

1. Blake, W. K. (1970), "Turbulent Boundary Layer Wall Pressure Fluctuations on Smooth and Rough Walls," J. Fluid Mech., 44, 4, 637-660.

2. Burton, T. E. (1973), "Wall Pressure Fluctuations at Smooth and Rough Surfaces Under Turbulent Boundary Layers with Favorable and Adverse Pressure Gradients," M.I.T. Acoustics and Vibration Lab. Report No. 70208-9.

3. Corcos, G. M. (1963), "Resolution of Pressure in Turbulence," J. Acoustical Society of America, 35, 192-199.

4. Davies, H. G. (1971), "Sound from Turbulent-Boundary-Layer-Excited Panels," J. Acoustical Society of America, Vol. 49, No. 3 (Part 2), 878-889.

5. Hanson, E. E. (1969), "The Design and Construction of a Low-Noise, Low-Turbulence Wind Tunnel," M.I.T. Acoustics and Vibration Lab. Report No. 79611-1.

6. Martin, N. C. and Leehey, P. (1976), "Low Wavenumber Wall Pressure Measurements Using a Rectangular Membrane as a Spatial Filter." (To be published)

7. Schloemer, H. H. (1966), "Effects of Pressure Gradients on Turbulent Boundary-Layer Wall-Pressure Fluctuations," USN Underwater Sound Lab. Report No. 747.

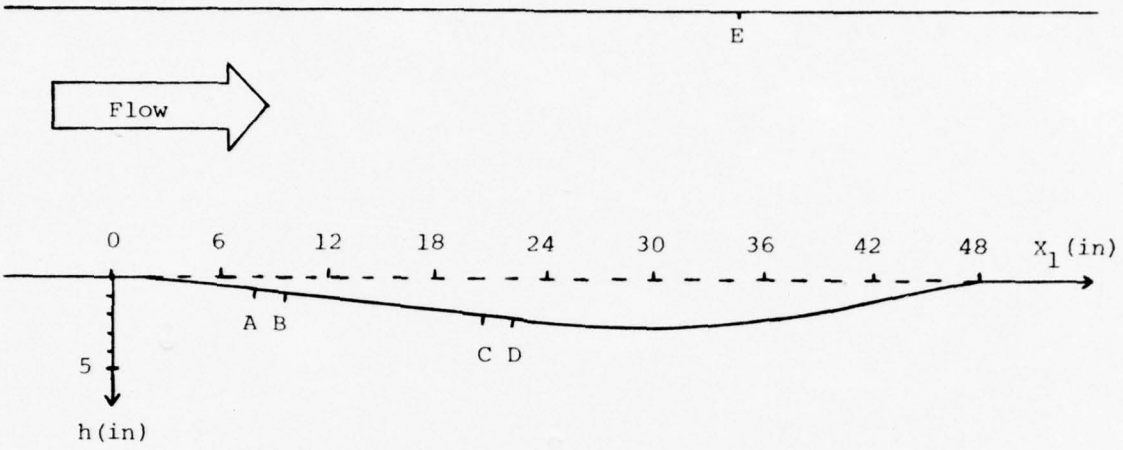

FIGURE 2.1 Profile of the bottom wall of the wind tunnel duct.

X(in)	0	3	6	9	12	15	18	21	24
h(in)	0.00	0.08	0.33	0.66	1.01	1.35	1.70	2.04	2.36
X(in)	27	30	33	36	39	42	45	48	
h(in)	2.56	2.60	2.50	2.20	1.79	1.22	0.54	0.00	

NOTE:
1. The profile is a straight line between A(8") and D(22").
2. The steel test plate was mounted flush between B(9.5") and C(20.5").
3. Pressure release holes provided at E on the top wall of the wind tunnel.

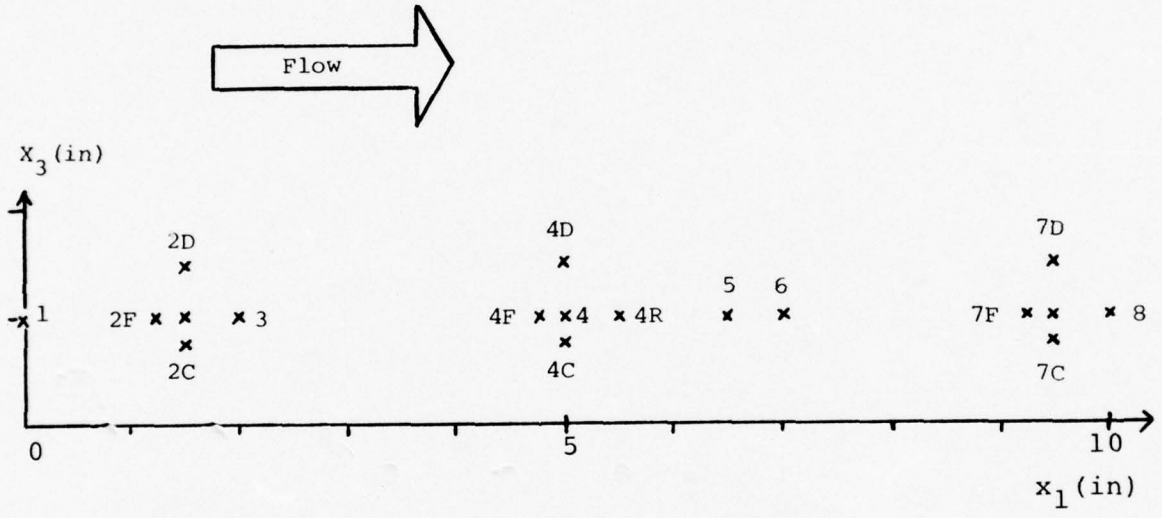

FIGURE 3.1 Measuring stations for flow properties

Note: Station 3 is also Station 2R.
Station 8 is also Station 7R.

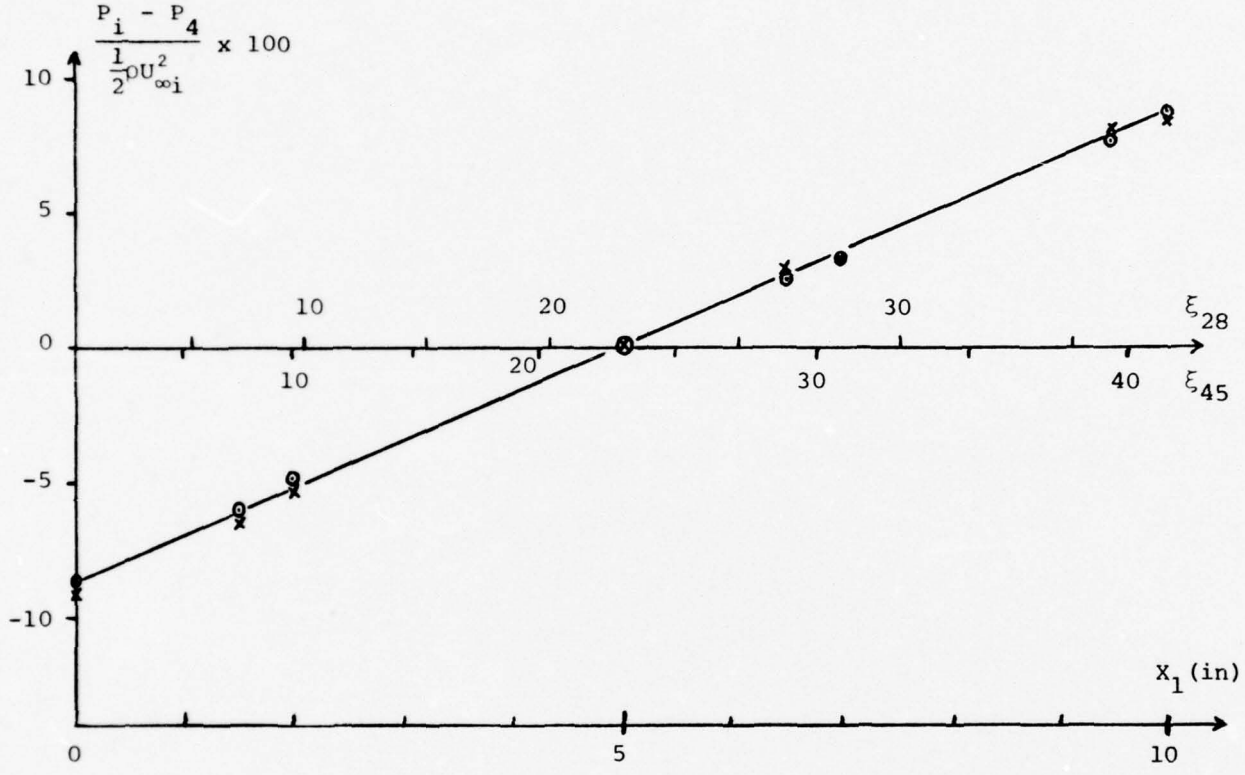

FUGURE 3.2 Static pressure profile. P_i = pressure at station #i

$U_{\infty i}$ is the mean flow velocity over station #i.

⊙: $U_\infty \approx$ 28 m/sec.

X: $U_\infty \approx$ 45 m/sec

ξ_j is defined by $dx_1 = \delta_j^*(X_1)d\xi_j$; and $\xi_j = 0$ at $X_1 = 0$. Also note that

ξ_{28}: $U_\infty \approx$ 28 m/sec;

ξ_{45}: $U_\infty \approx$ 48 m/sec.

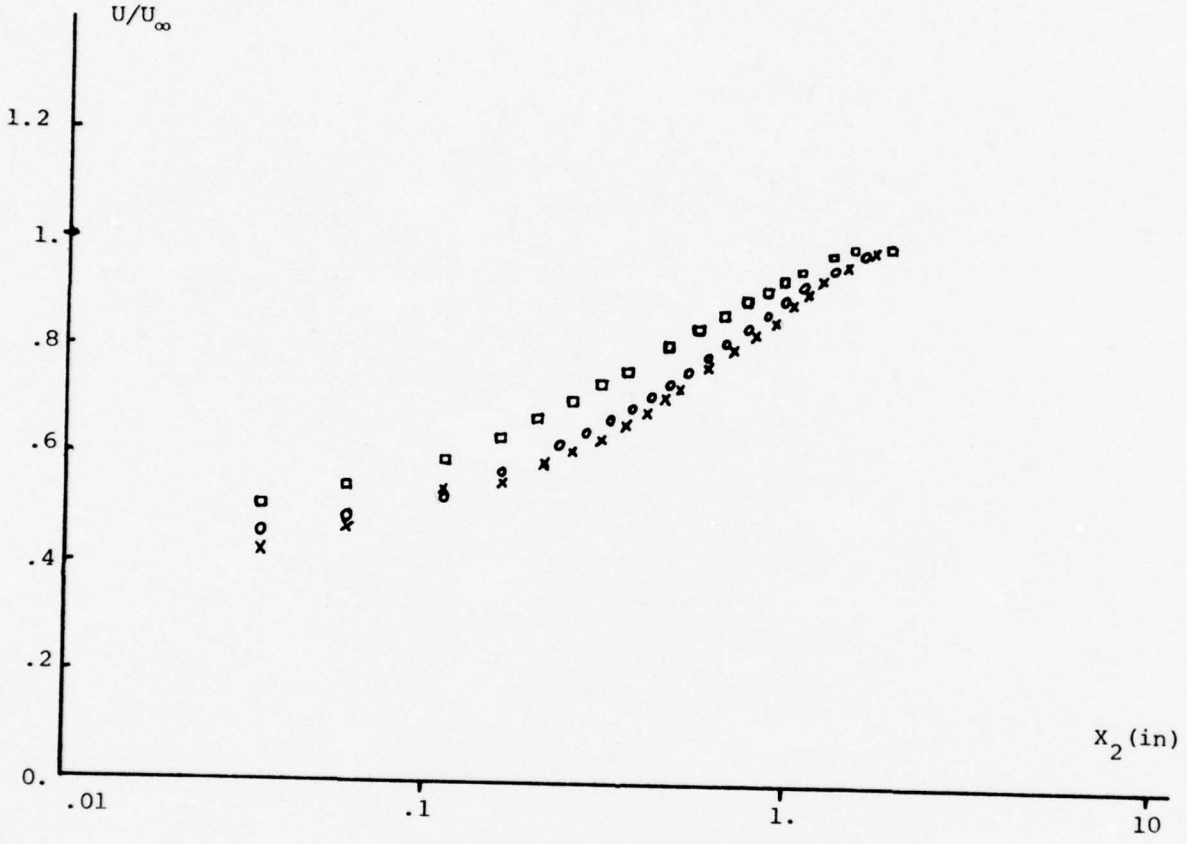

FIGURE 3.3a Boundary layer velocity profile, $U_\infty \approx 28$ m/sec.

□ : ξ = 7.1

O: ξ = 28.1

X: ξ = 36.3

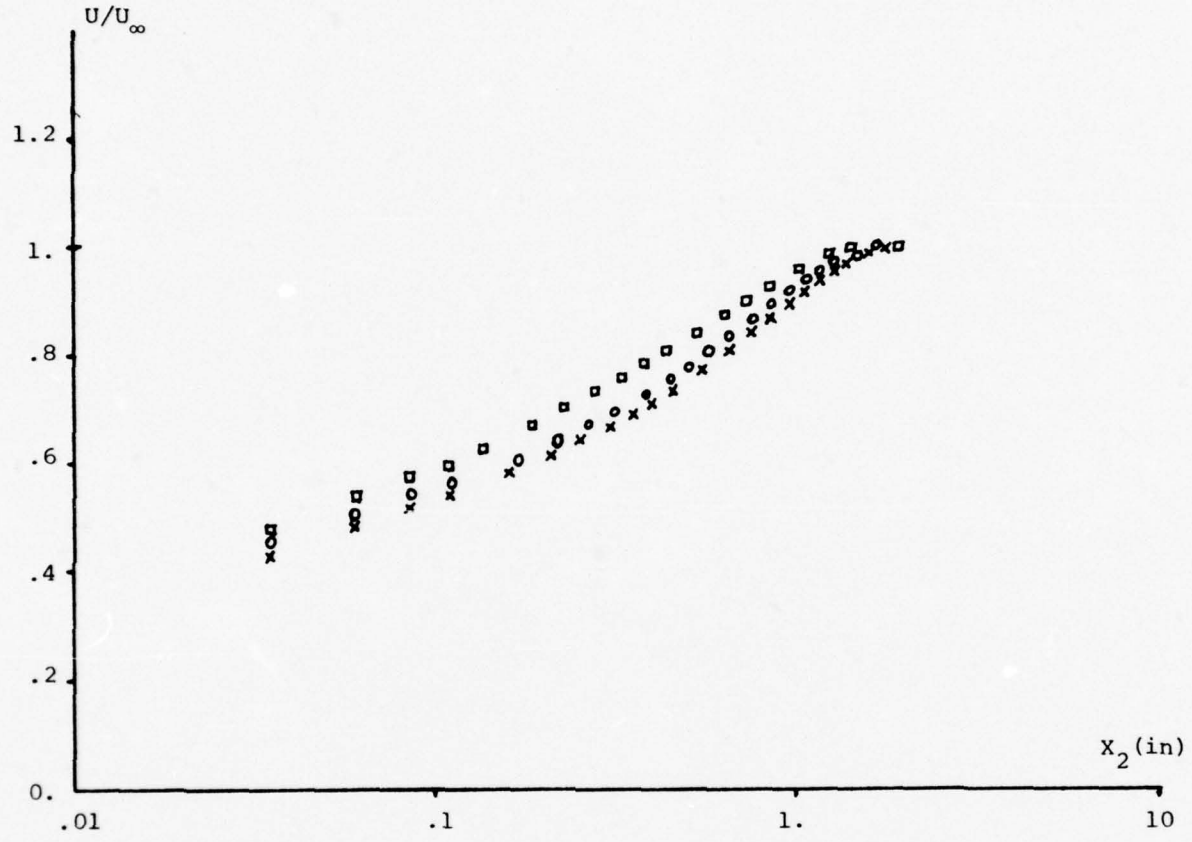

FIGURE 3.3b Boundary layer velocity profile, $U_\infty \simeq 45$ m/sec.

□ : $\xi = 7.1$

O : $\xi = 28.1$

X : $\xi = 36.3$

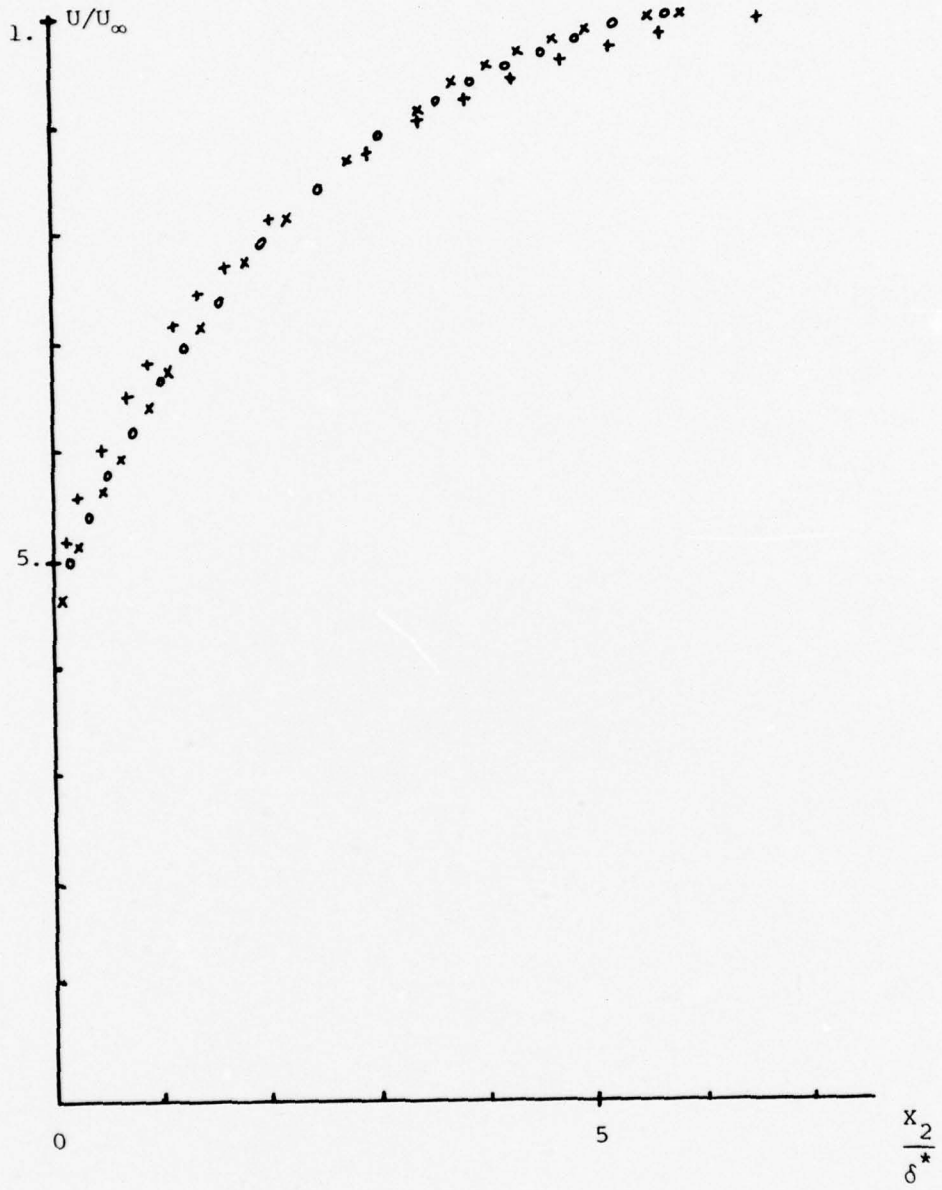

FIGURE 3.4a Mean flow velocity profile, $U_\infty \approx 28$ m/sec

+: $\xi = 7.1$

O: $\xi = 28.1$

X: $\xi = 36.3$

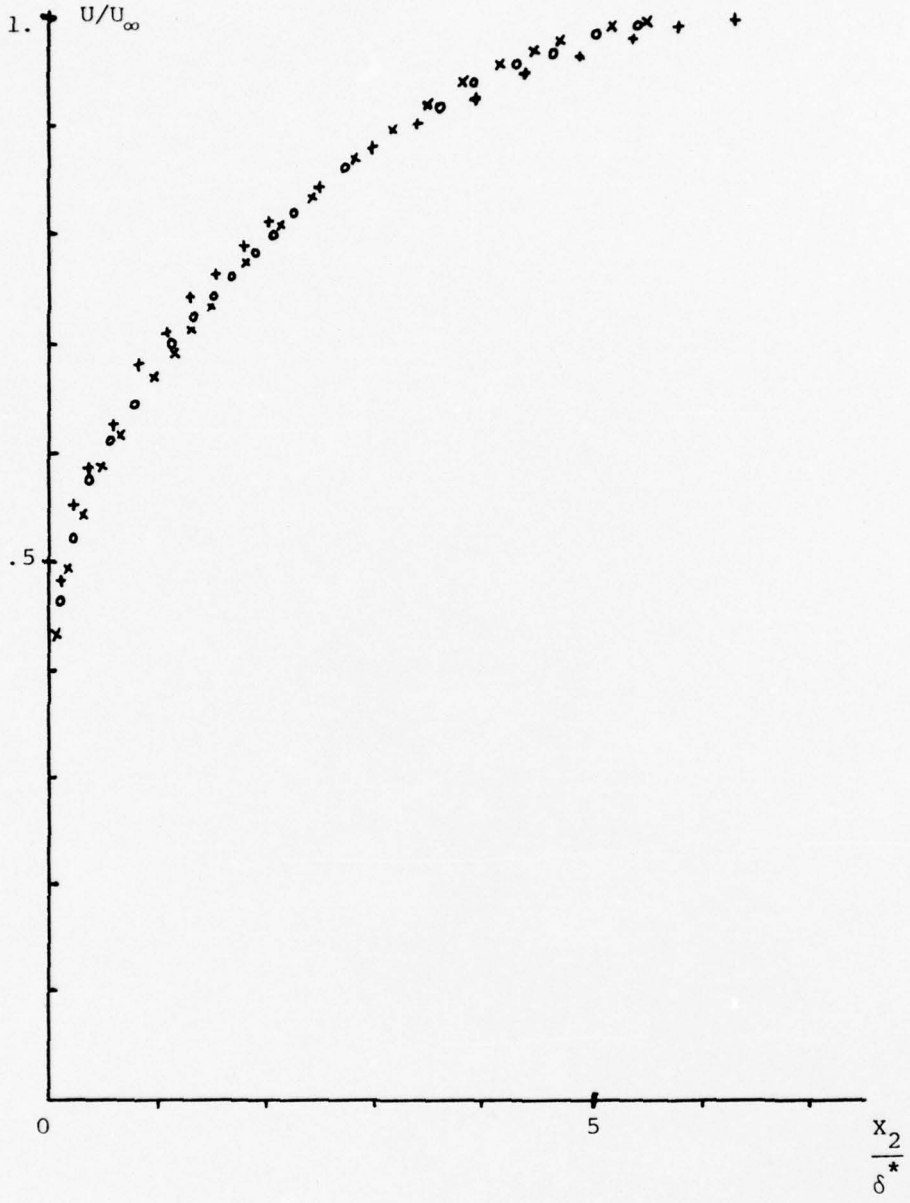

FIGURE 3.4b Mean flow velocity profile, $U_\infty \tilde{} 45$ m/sec

+: $\xi = 7.5$

O: $\xi = 30.7$

X: $\xi = 39.6$

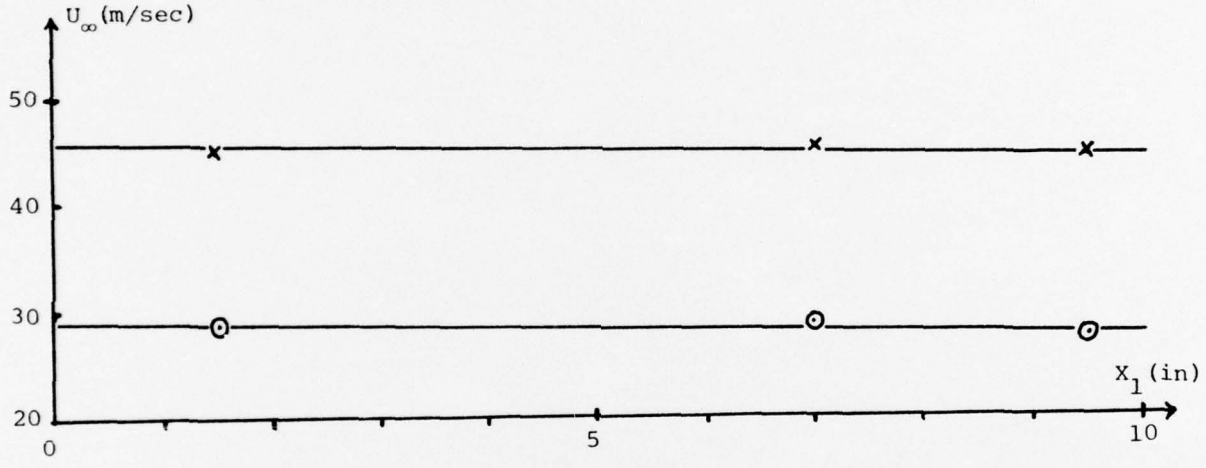

FIGURE 3.5 Mean flow velocity

⊙: $U_\infty \approx 28$ m/sec

X: $U_\infty \approx 45$ m/sec

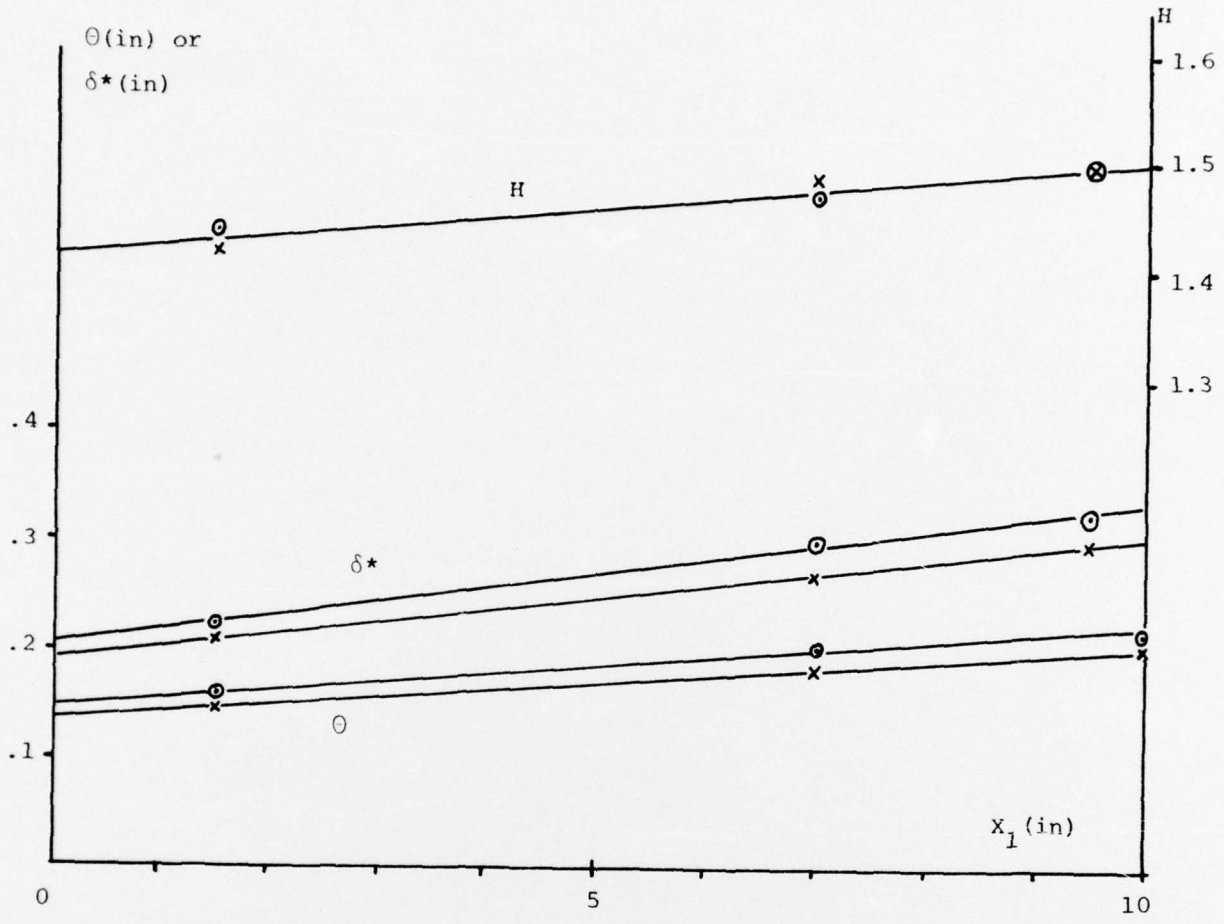

FIGURE 3.6 Displacement thickness, δ^*; momentum thickness, Θ; and shape factor, H.

Θ: $U_\infty \approx 28$ m/sec

X: $U_\infty \approx 45$ m/sec

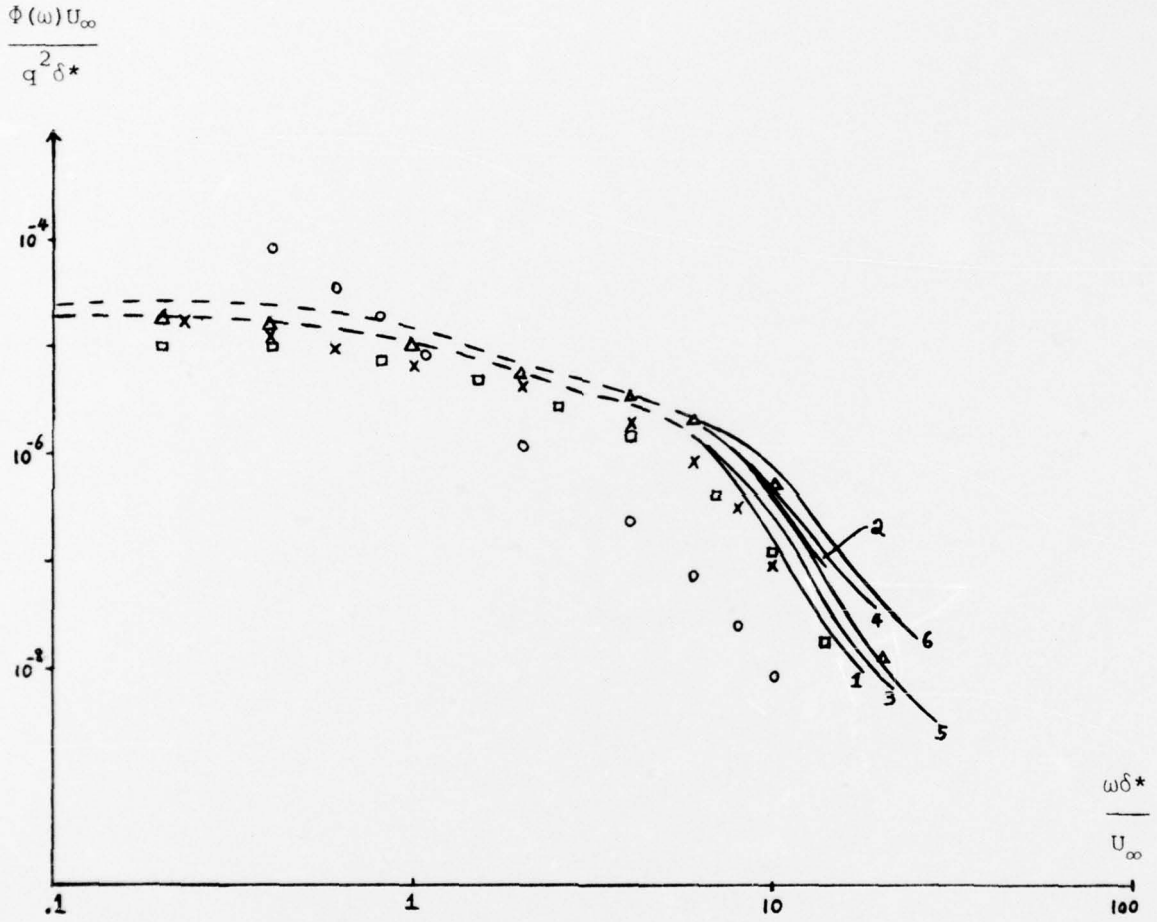

FIGURE 3.7 Wall pressure power spectra.

Curve	U_∞(m/sec)	ξ
1	28	7.1
2	45	7.5
3	28	28.1
4	45	30.7
5	28	36.3
6	45	39.6

Curves 1, 2, 3, 4, 5, 6 are bounded within the dash lines for $\omega\delta^*/U_\infty < 7$.

Δ: Blake (1970) $\partial p/\partial x = 0$.

$\square$: Burton (1973) $\xi = 0$, $\partial p/\partial x > 0$

o: Burton (1973) $\xi = 24.6$, $\partial p/\partial x > 0$

x: Burton (1973) $\partial p/\partial x = 0$

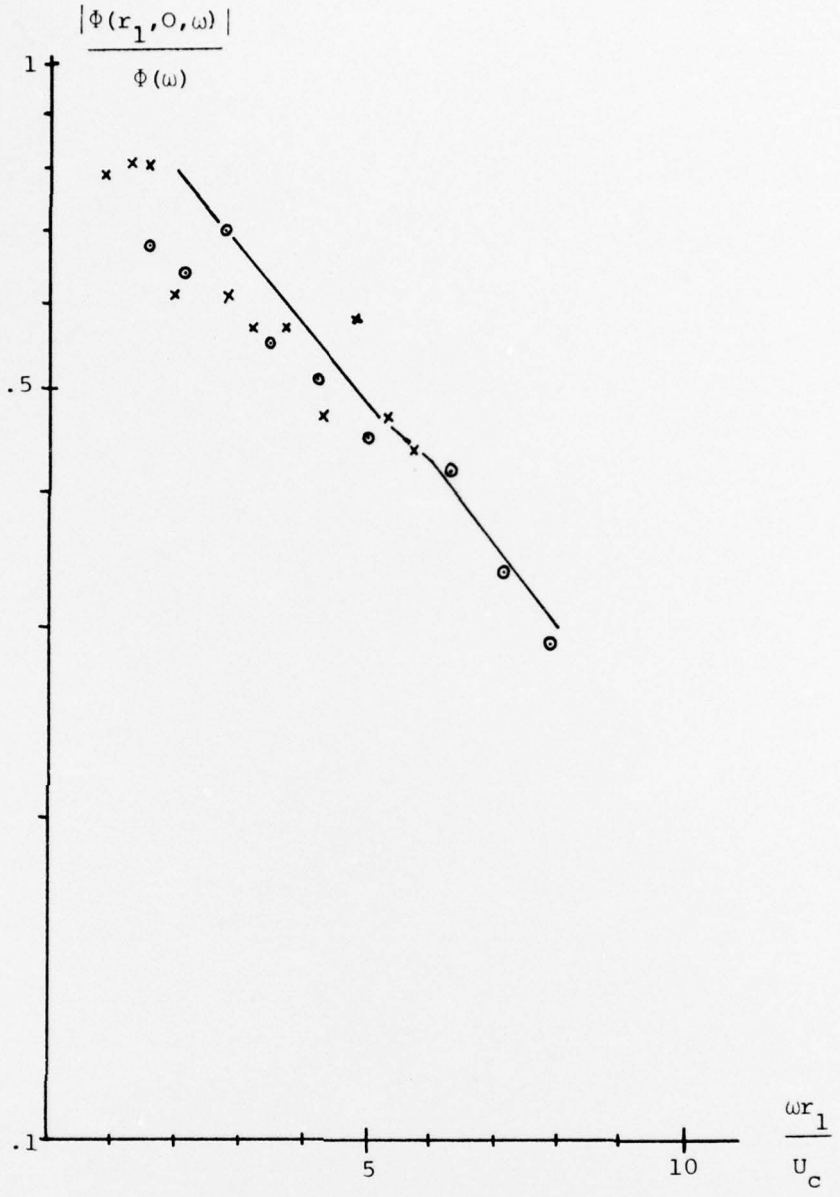

FIGURE 3.8a Longitudinal cross spectral densities

Probe stations: 2F & 2R

⊙: $U_\infty \approx 28$ m/sec

X: $U_\infty \approx 45$ m/sec

—: Schloemer (1966)

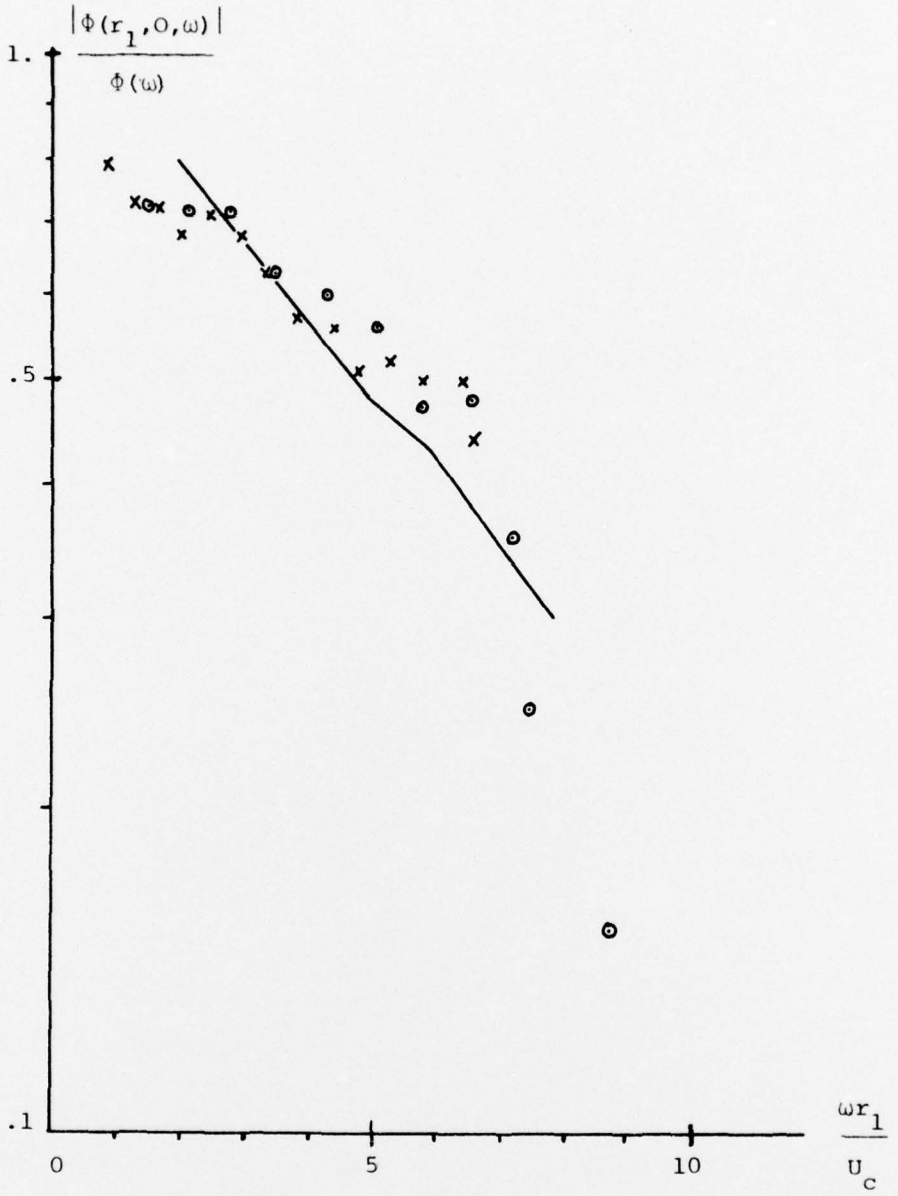

FIGURE 3.8b Longitudinal cross spectral densities

(Probe stations: 4F & 4R)

⊙: $U_\infty \approx 28$ m/sec

X: $U_\infty \approx 45$ m/sec

—: Schloemer (1966)

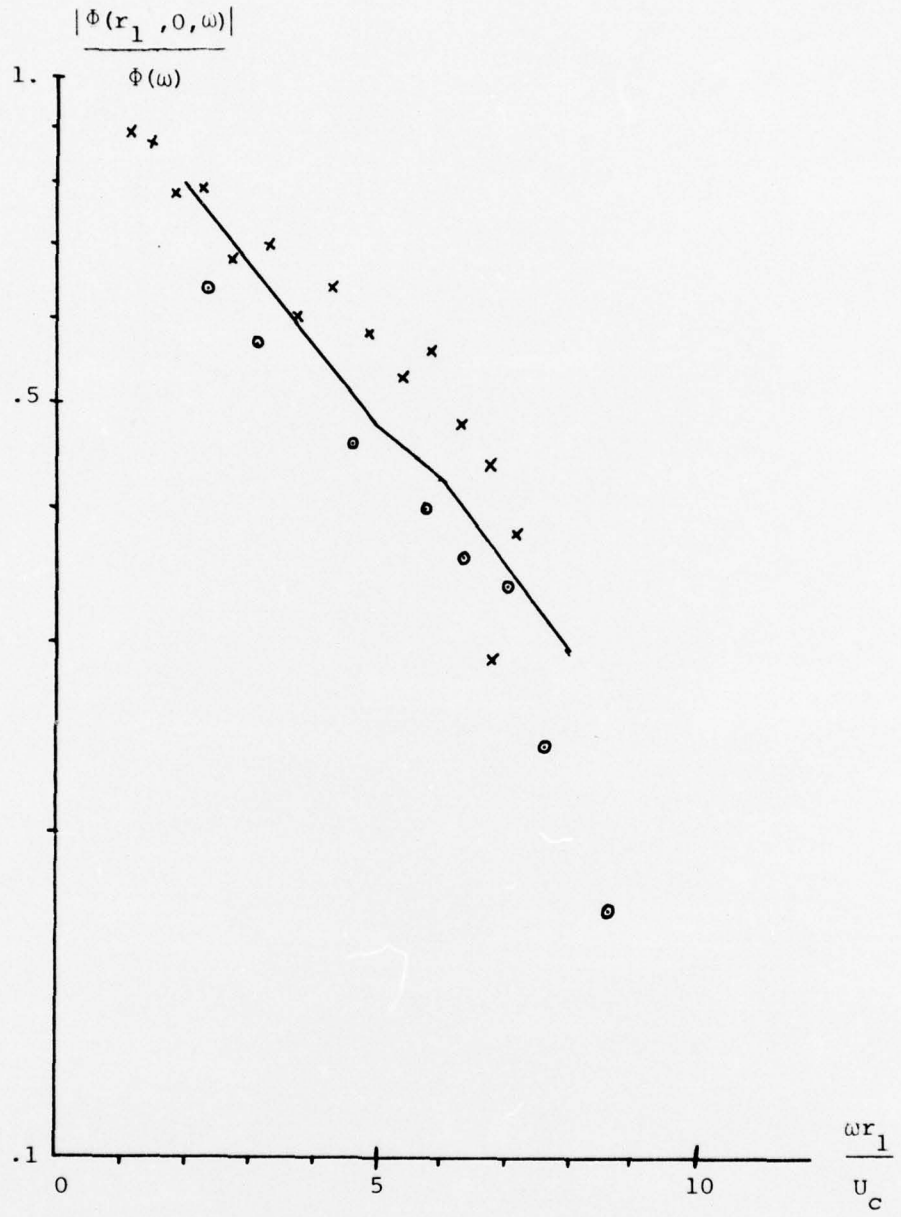

FIGURE 3.8c Longitudinal cross spectral density

(Probe stations: 7F & 7R)

⊙: $U_\infty \approx$ 28 m/sec

X: $U_\infty \approx$ 45 m/sec

—: Schloemer (1966)

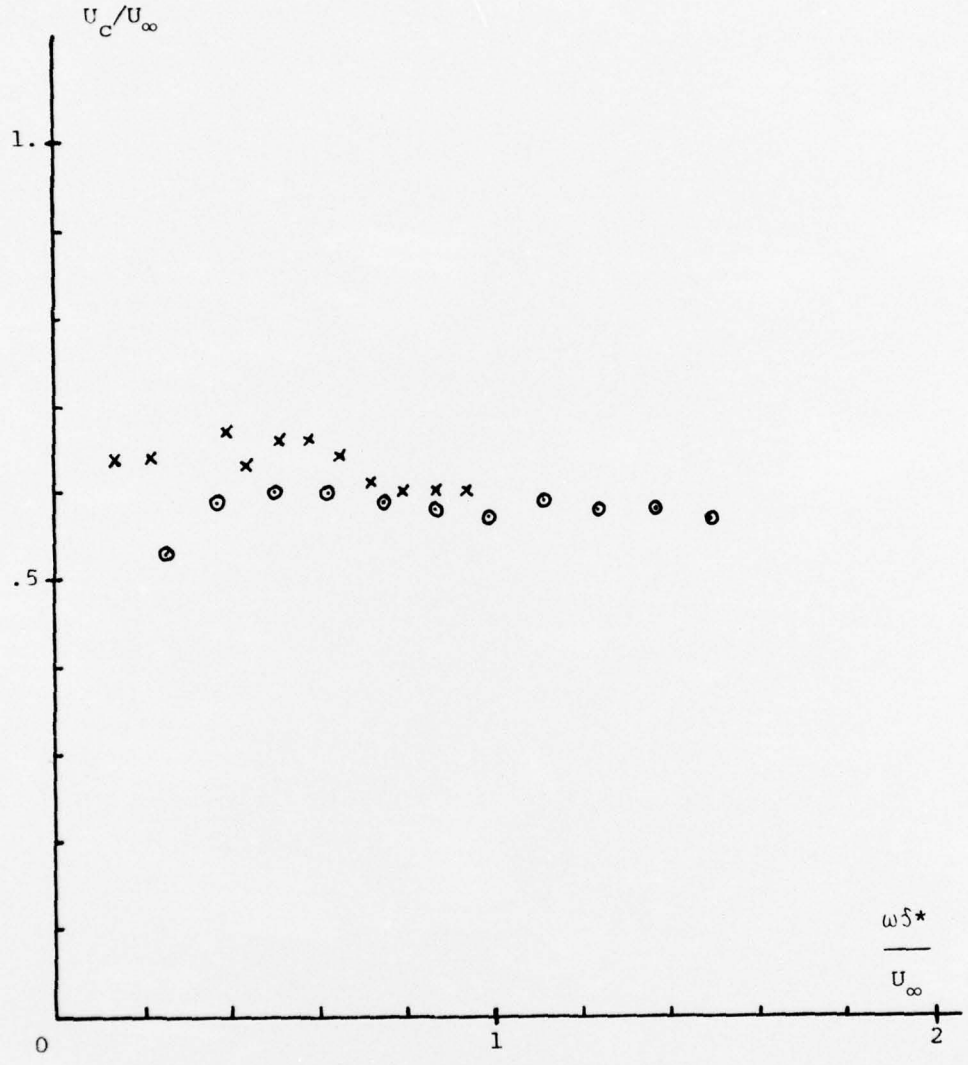

FIGURE 3.9a Convection velocities

(Probe stations: 2F & 2R)

⊙: $U_\infty \approx 28$ m/sec

X: $U_\infty \simeq 45$ m/sec

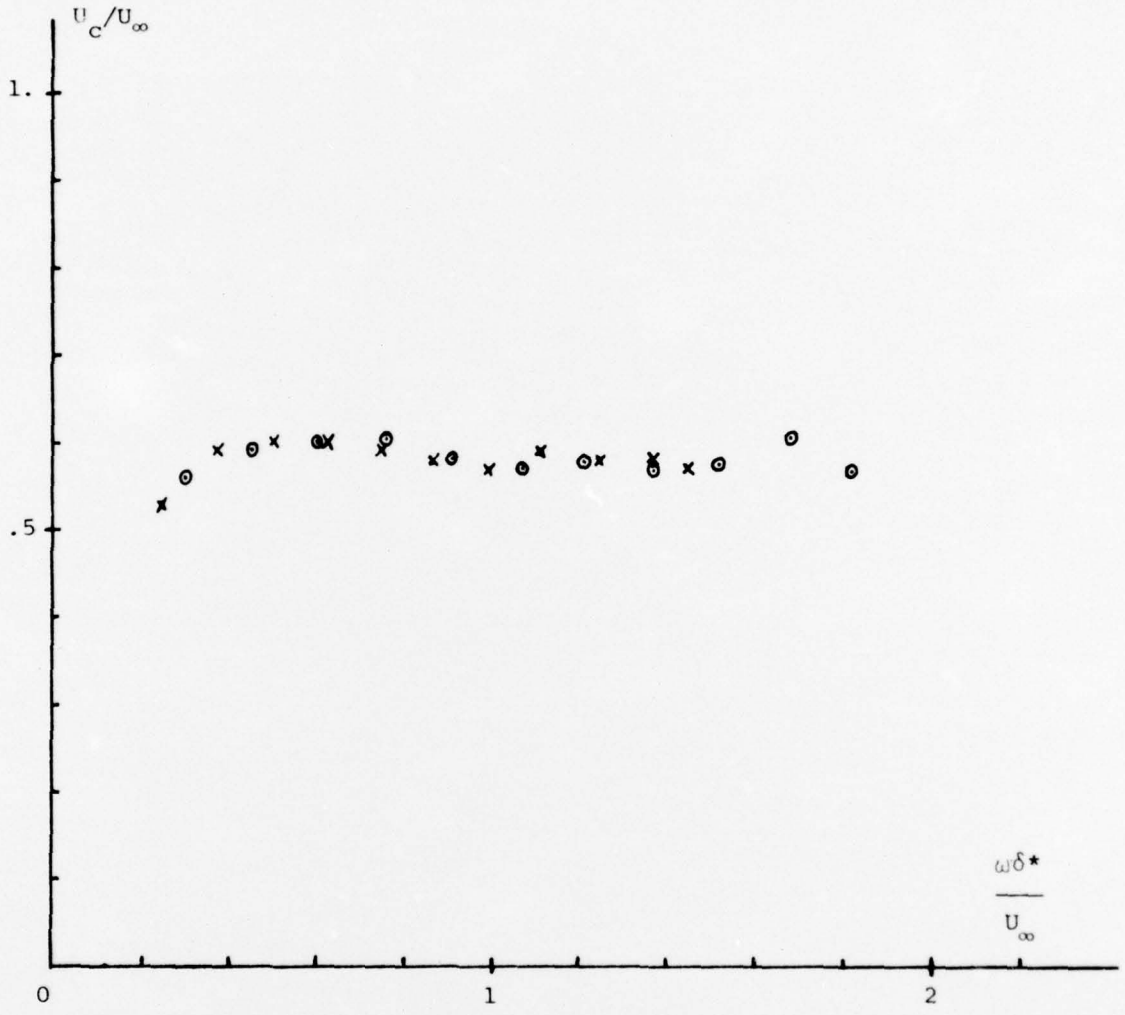

FIGURE 3.9b Convention velocities

(Probe stations: 4F & 4R)

⊙: $U_\infty \simeq 28$ m/sec

X: $U_\infty \simeq 45$ m/sec

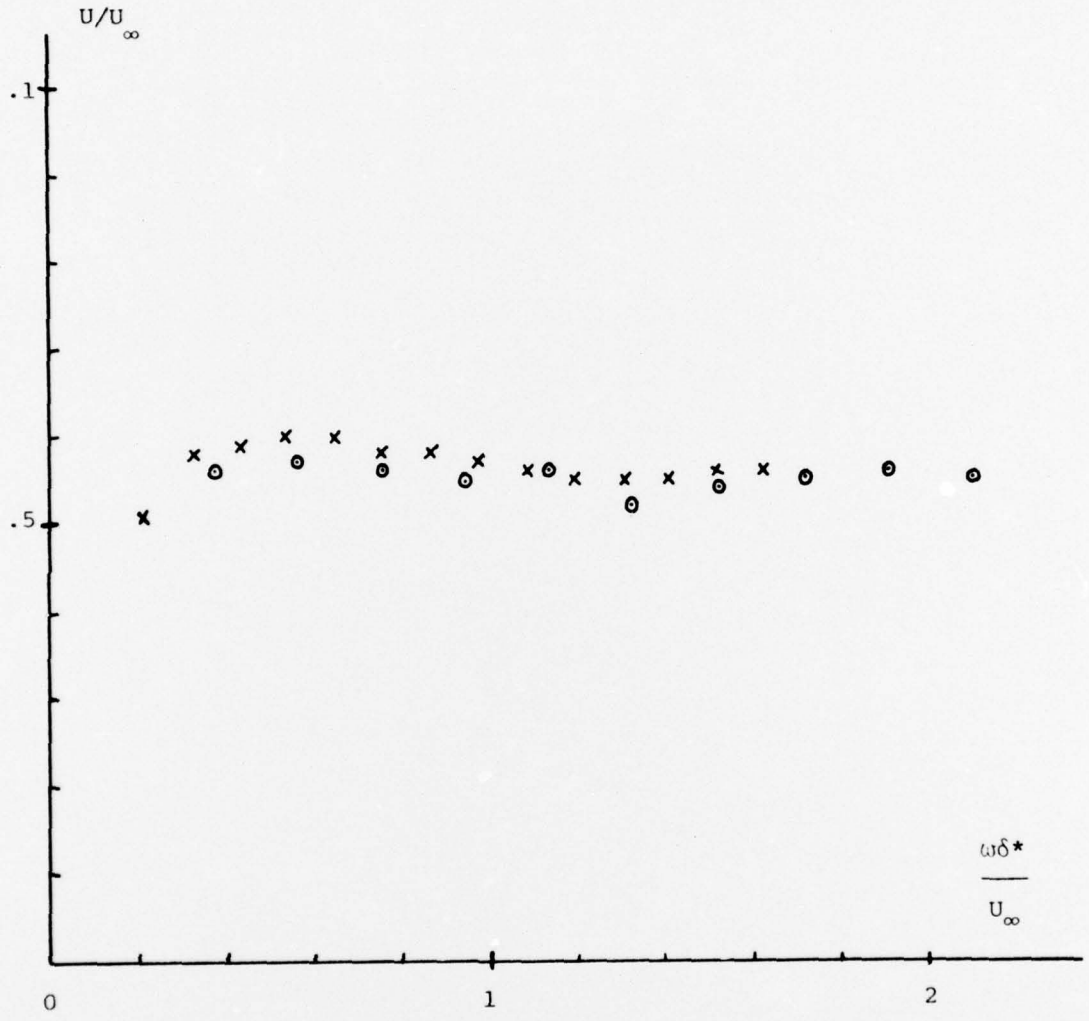

FIGURE 3.9c Convection velocities

(Probe stations: 7F & 7R)

⊙: $U_\infty \simeq 28$ m/sec

X: $U_\infty \simeq 45$ m/sec

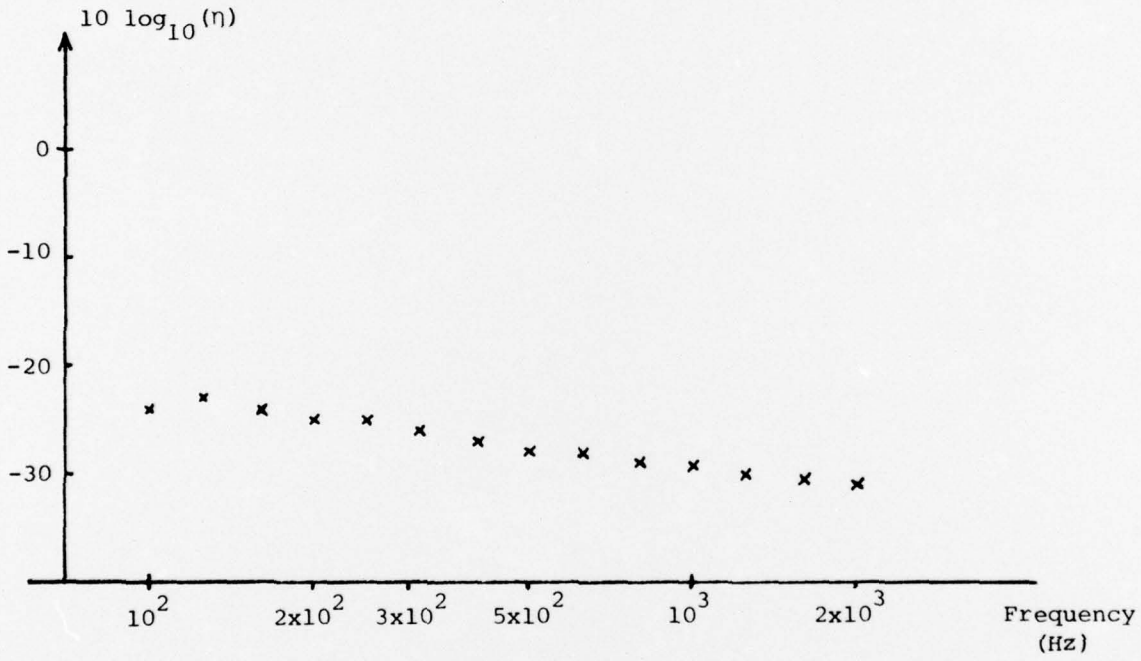

FIGURE 4.1 Loss factor, η, of steel test plate.
Plate thickness is .003"

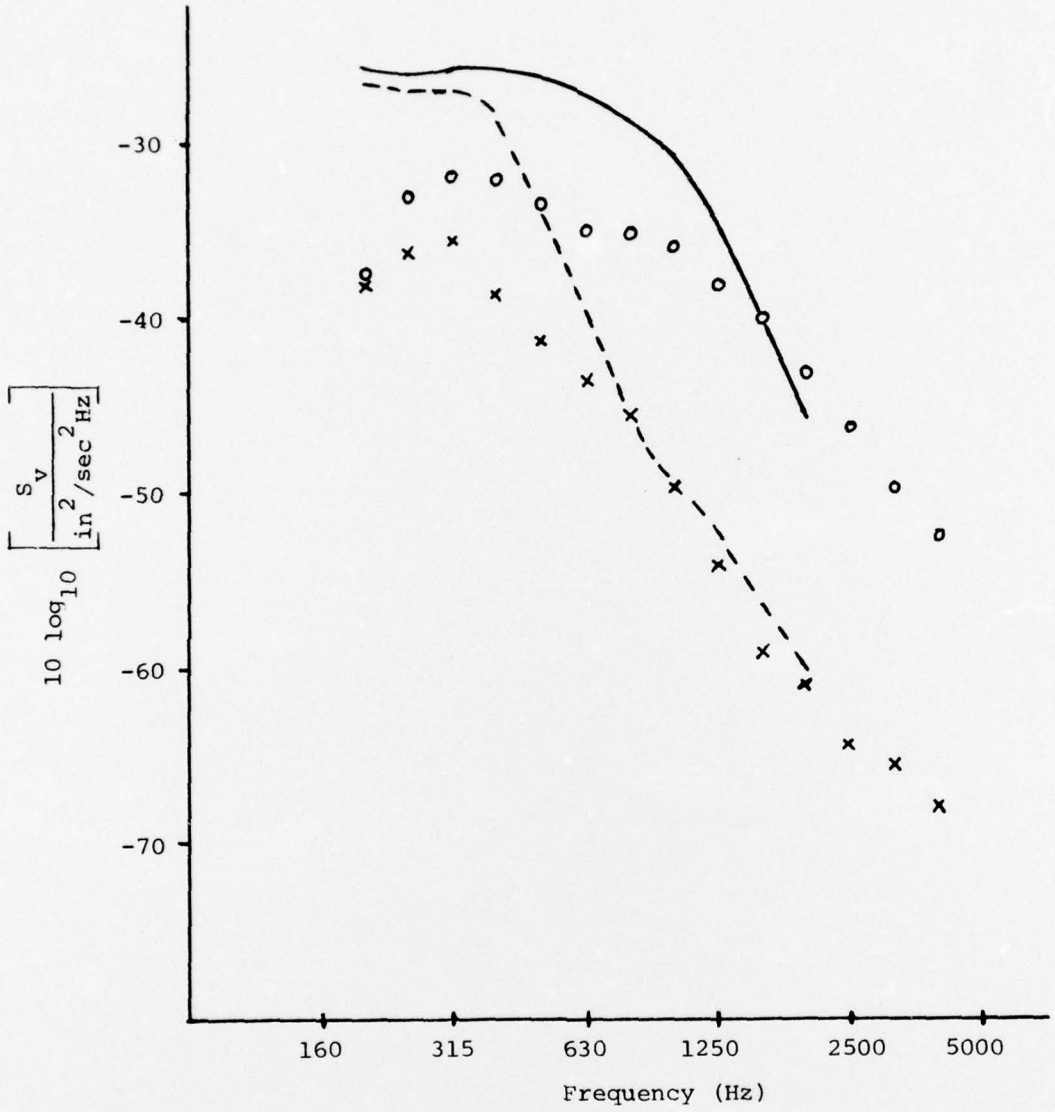

FIGURE 4.2 Vibration levels of steel test plate

x: $U_\infty \simeq$ 28 m/sec, experimental
--: $U_\infty \simeq$ 28 m/sec, analytical
o: $U_\infty \simeq$ 45 m/sec, experimental
—: $U_\infty \simeq$ 45 m/sec, analytical

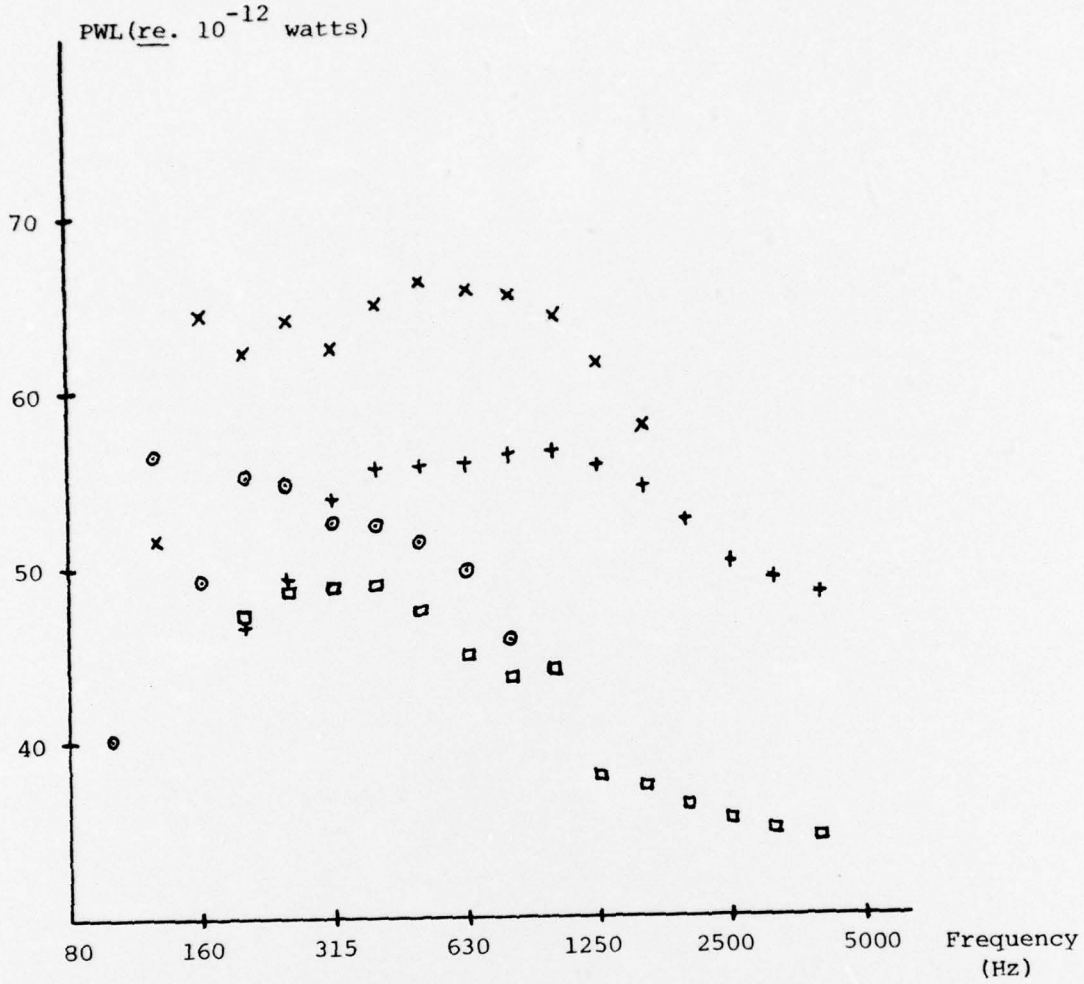

FIGURE 4.3 Radiated sound power levels, PWL, in one third octave bands.

U_∞ (m/sec)

x: $U_\infty \approx 45$ m/sec } deduced from sound
o: $U_\infty \approx 28$ m/sec } pressure levels, SPL

+: $U_\infty \approx 45$ m/sec } predicted from measured vibration
□: $U_\infty \approx 29$ m/sec } levels, $V(\omega)$

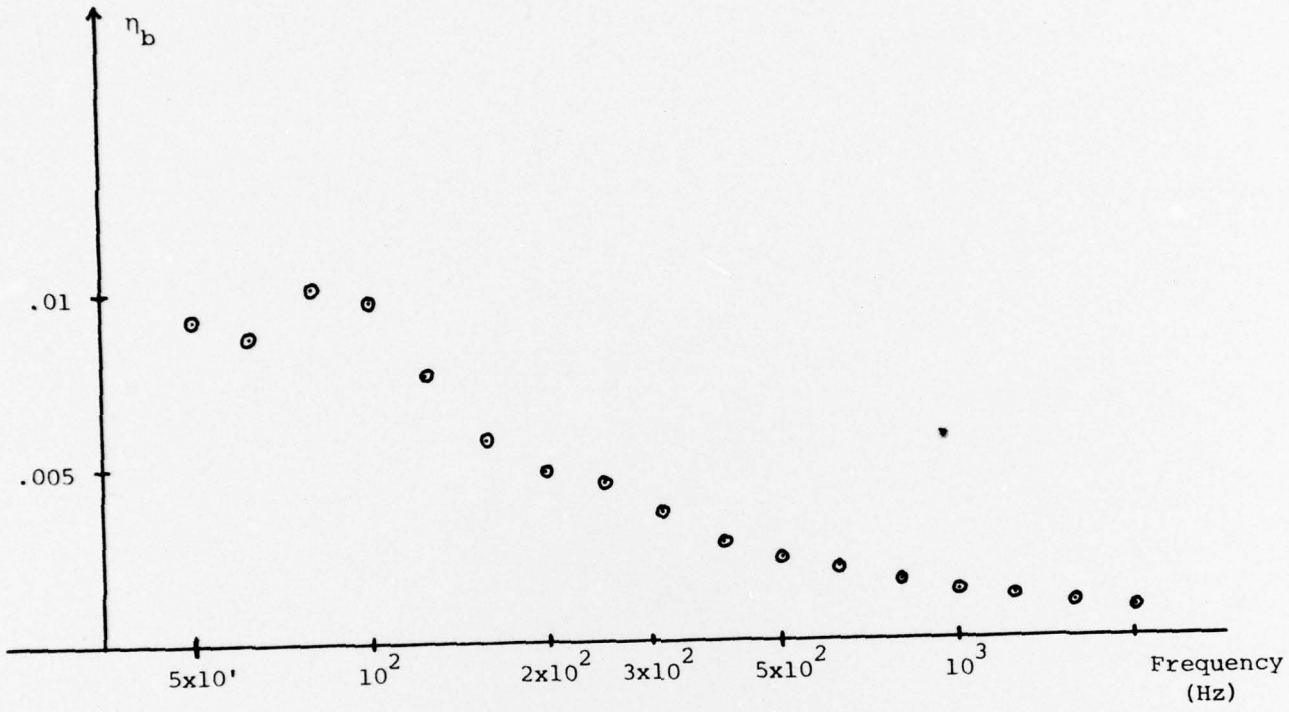

FIGURE 4.4 Acoustic loss factor, η_b, of reverberant blockhouse enclosing the test section.

M.I.T., A & V Report 70208-12

Vibration of and Acoustic Radiation from a Panel Excited by Adverse Pressure Gradient Flow, by Yi Mason Chang and Patrick Leehey, May 1976, 35 pgs., illustrated. UNCLASSIFIED

Flow with uniform adverse pressure gradient was created over the surface of a steel test plate. Vibration velocity levels on the plate and acoustic radiation from the plate were measured and compared with theoretical estimates. The measured vibration levels agree with theory for frequencies above those for hydrodynamic coincidence. Below these frequencies theoretical predictions of vibration levels are too high, but theoretical predictions of radiated sound power, based on measured vibration levels, are too low. Possible reasons for these compensating errors are discussed.

Boundary Layer Noise

Plate Vibration

Acoustic Radiation

Wall Pressure Fluctuation

Adverse Pressure Gradient

M.I.T., A & V Report 70208-12

Vibration of and Acoustic Radiation from a Panel Excited by Adverse Pressure Gradient Flow, by Yi Mason Chang and Patrick Leehey, May 1976, 35 pgs., illustrated. UNCLASSIFIED

Flow with uniform adverse pressure gradient was created over the surface of a steel test plate. Vibration velocity levels on the plate and acoustic radiation from the plate were measured and compared with theoretical estimates. The measured vibration levels agree with theory for frequencies above those for hydrodynamic coincidence. Below these frequencies theoretical predictions of vibration levels are too high, but theoretical predictions of radiated sound power, based on measured vibration levels, are too low. Possible reasons for these compensating errors are discussed.

Boundary Layer Noise

Plate Vibration

Acoustic Radiation

Wall Pressure Fluctuation

Adverse Pressure Gradient

M.I.T., A & V Report 70208-12

Vibration of and Acoustic Radiation from a Panel Excited by Adverse Pressure Gradient Flow, by Yi Mason Chang and Patrick Leehey, May 1976, 35 pgs., illustrated. UNCLASSIFIED

Flow with uniform adverse pressure gradient was created over the surface of a steel test plate. Vibration velocity levels on the plate and acoustic radiation from the plate were measured and compared with theoretical estimates. The measured vibration levels agree with theory for frequencies above those for hydrodynamic coincidence. Below these frequencies theoretical predictions of vibration levels are too high, but theoretical predictions of radiated sound power, based on measured vibration levels, are too low. Possible reasons for these compensating errors are discussed.

Boundary Layer Noise

Plate Vibration

Acoustic Radiation

Wall Pressure Fluctuation

Adverse Pressure Gradient

M.I.T., A & V Report 70208-12

Vibration of and Acoustic Radiation from a Panel Excited by Adverse Pressure Gradient Flow, by Yi Mason Chang and Patrick Leehey, May 1976, 35 pgs., illustrated. UNCLASSIFIED

Flow with uniform adverse pressure gradient was created over the surface of a steel test plate. Vibration velocity levels on the plate and acoustic radiation from the plate were measured and compared with theoretical estimates. The measured vibration levels agree with theory for frequencies above those for hydrodynamic coincidence. Below these frequencies theoretical predictions of vibration levels are too high, but theoretical predictions of radiated sound power, based on measured vibration levels, are too low. Possible reasons for these compensating errors are discussed.

Boundary Layer Noise

Plate Vibration

Acoustic Radiation

Wall Pressure Fluctuation

Adverse Pressure Gradient